NASA Contractor Report 178230

ICASE REPORT NO. 87-1

ICASE

MULTIGRID APPLIED TO SINGULAR PERTURBATION PROBLEMS

(NASA-CR-178230) MULTIGRID APPLIED TO SINGULAR PERTURBATION PROBLEMS Final Report (NASA) 28 p CSCL 09b

N87-17444

Unclas
G3/61 44012

David Kamowitz

Contract No. NAS1-18107

January 1987

INSTITUTE FOR COMPUTER APPLICATIONS IN SCIENCE AND ENGINEERING
NASA Langley Research Center, Hampton, Virginia 23665

Operated by the Universities Space Research Association

National Aeronautics and
Space Administration

Langley Research Center
Hampton, Virginia 23665

Multigrid Applied to Singular Perturbation Problems

David Kamowitz*

Abstract

The solution of the singular perturbation problem

$$-\varepsilon u'' + b(x)u' = f, \qquad 0 < x < 1$$

with

$$1 \gg \varepsilon > 0, \quad u(0) = u_0, \quad u(1) = u_1$$

by a multigrid algorithm is considered. Theoretical and experimental results for a number of different discretizations are presented. The theoretical and observed rates agree with the results developed in an earlier work of Kamowitz and Parter.

In addition, the rate of convergence of the algorithm when the coarse grid operator is the natural finite difference analogue of the fine grid operator is presented. This is in contrast to the case in the previous work where the Galerkin choice ($I_h^H L_h I_H^h$) was used for the coarse grid operators.

*Supported by the U.S. Air Force Office of Scientific Research under Contract No. AFOSR-82-0275. Additional support was provided by the National Aeronautics and Space Administration under NASA Contract No. NAS1-18107 while in residence at the Institute for Computer Applications in Science and Engineering, ICASE, NASA Langley Research Center, Hampton, VA 23665-5225.

1 Introduction

This report discusses the application of a multigrid algorithm to the solution of the following one dimensional singular perturbation problem:

$$-\varepsilon u'' + b(x)u' = f, \qquad 0 < x < 1 \tag{1}$$

with

$$1 \gg \varepsilon > 0, \qquad u(0) = u_0, \quad u(1) = u_1.$$

Many other authors have discussed the application of various methods of solution to the algebraic problem; in particular see Dorr [Dorr70a], Babuska [Babu69a], Ervin and Layton [Ervi85a], and Kellogg and Tsan [Kell78a].

Much of the literature regarding multigrid methods restricts itself to the solution of *nice* problems. Indeed most authors require that the linear system be well conditioned in addition to symmetric and positive definite. However, in the case of singular perturbation problems as the coefficient of the second order term tends to zero the usual symmetric discretization fails to be of positive type. Thus the first measure taken in the numerical discretization of these problems is to replace the usual symmetric difference of the first order term with some form of skewed differencing. In particular for problems with turning points this may lead to a system of equations which is ill–conditioned for small ε.

From the standpoint of calculating a numerical approximation to the solution of problem (1) the first question is: does the discretization converge to the continuous solution? Then, assuming it does, how does the multigrid algorithm perform as a solver for this system of linear equations? What modifications, if any, are necessary in the multigrid algorithm?

The main result shows that if the original system of equations resulting from the discretization of problem (1) is of positive type then the theoretical results for the multigrid algorithm developed in Kamowitz and Parter [Kamo85a] and in McCormick and Ruge [McCo82a] apply.

From a computational perspective it is convenient to use for the coarse grid operators of the multigrid algorithm the operators that are the finite difference analogue of the original operator. In Section 6 the rate of convergence of the algorithm using the finite difference version of the coarse grid operators is considered. It is shown that the new rate of convergence is an $O(h^2)$ perturbation of the rate obtained using the Galerkin choice.

2 The Discrete Problem

Three model problems are chosen for study, one where the sign of $b(x)$ does not change and two where $b(x)$ changes sign. The three problems are designated

Problem BL

$$Lu \equiv -\varepsilon u'' + u' = 0, \qquad 0 < x < 1 \tag{2}$$

Problem TP-1

$$Lu \equiv -\varepsilon u'' + (x - \frac{1}{2})u' = 0, \qquad 0 < x < 1 \tag{3}$$

Problem TP-2

$$Lu \equiv -\varepsilon u'' - (x - \frac{1}{2})u' = 0 \qquad 0 < x < 1. \tag{4}$$

For all three problems the boundary conditions are

$$u(0) = 1, \qquad u(1) = 3.$$

For the discrete problem as usual let $N > 0$ be chosen and set $h = 1/(N+1)$. The interval

$$\Omega = (0, 1)$$

is discretized to form

$$\Omega_h \equiv \{ih : 1 \le i \le N\}.$$

The notation x_i refers to the point ih and u_i refers to $u(x_i)$. In addition the usual notation for finite differences is used:

$$D_+ u_i = \frac{u_{i+1} - u_i}{h}, \qquad D_- u_i = \frac{u_i - u_{i-1}}{h}$$

$$D_0 u_i = \frac{u_{i+1} - u_{i-1}}{2h}, \qquad D_+ D_- u_i = \frac{u_{i+1} - 2u_i + u_{i-1}}{h^2}$$

For problem (BL) the following two discretizations are considered:

$$L_h^1 u_i \equiv -\varepsilon D_+ D_- u_i + D_- u_i \qquad \text{(upwind differencing)}$$

$$L_h^2 u_i \equiv \frac{-\varepsilon}{1 + h/2\varepsilon} D_+ D_- u_i + D_- u_i \qquad \text{(see Kellogg and Tsan).}$$

Since problems (*TP-1*) and (*TP-2*) have turning points at $x = \frac{1}{2}$ it is necessary to change the direction of the discretization of the first order term. For problem (*TP-1*) the discretization tested is

$$L_h^3 u_i \equiv -\varepsilon D_+ D_- u_i + (x_i - \tfrac{1}{2}) D_+ u_i, \qquad 1 \le i \le \frac{N+1}{2} \tag{5}$$

$$L_h^3 u_i \equiv -\varepsilon D_+ D_- u_i + (x_i - \tfrac{1}{2}) D_- u_i, \qquad \frac{N+1}{2} + 1 \le i \le N. \tag{6}$$

Similarly, for problem (*TP-2*) the discretization is

$$L_h^4 u_i \equiv -\varepsilon D_+ D_- u_i - (x_i - \tfrac{1}{2}) D_- u_i, \qquad 1 \le i \le \frac{N+1}{2} \tag{7}$$

$$L_h^4 u_i \equiv -\varepsilon D_+ D_- u_i - (x_i - \tfrac{1}{2}) D_+ u_i, \qquad \frac{N+1}{2} + 1 \le i \le N. \tag{8}$$

Note that each of the discretizations L_h^k, $k = 1, \ldots, 4$ results in a tridiagonal linear system of equations whose coefficient matrix may be denoted by

$$L_h^k \equiv [\ -\alpha_i \quad \beta_i \quad -\gamma_i\ ],$$

with

$$\alpha_i \ge 0, \quad \gamma_i \ge 0, \quad \text{and} \quad \beta_i \ge \alpha_i + \gamma_i.$$

Thus each L_h^k, $k = 1, \ldots, 4$ is an M–matrix and the linear system of equations

$$L_h^k u_i = f_i, \qquad 1 \le i \le N,$$

u_0 and u_{N+1} fixed has a solution; see for example Berman and Plemmons [Berm79a].

3 Review of the Multigrid Algorithm

The particular multigrid algorithm used to solve (1) has been discussed in detail in Kamowitz and Parter [Kamo85a]; thus only a cursory review is given here. In particular the details of the theory behind the convergence results can be found there. What is important to realize is that although the algorithm and convergence results discussed in the previous work apply to well conditioned two point boundary value problems the same bounds on the rate of convergence apply to the singular perturbation problems discussed here.

In order to completely describe the algorithm a number of spaces and operators need to be defined. For the various spaces choose g nested grids

$$\Omega_h \supset \Omega_{2h} \supset \ldots \supset \Omega_{ph}$$

where

$$p = 2^{g-1}.$$

Denote by S_{kh} the space of grid functions defined on Ω_{kh}. From now on the notation kh will be replaced by k. Denote by G_k the smoother, I_k^{k+1} the restriction map, and I_{k+1}^k the interpolation map. Associated with each space S_k there is also a nonsingular tridiagonal operator

$$L_k : S_k \mapsto S_k,$$

where L_k is of positive type. The operators L_k are again denoted

$$L_k = [\ -\alpha_i^k \quad \beta_i^k \quad -\gamma_i^k\ ].$$

These operators will be formally defined after the statement of the algorithm.

The following is an outline of the algorithm used. Assuming U_1^n is the nth approximation to the solution of the system of equations

$$L_1 U_1 = F_1$$

algorithm $MG(U_k^n, L_k, F_k, k)$ returns U_k^{n+1}, the next iteration of the multigrid algorithm. The grid layer is denoted by k; set $k = 1$ to start the algorithm on the finest grid layer.

Algorithm $MG(U_k^n, L_k, F_k, k)$

1. **Coarse Solve:** If $k = g$ (coarsest grid) then return
   $MG \leftarrow {L_g}^{-1} F_g$

otherwise

2. **Smooth:** Apply the smoother, G_k, call the result of this step $\tilde{U}_k^n$.
   If $k = 1$ use U_1^n as the initial guess, otherwise use 0.
3. **Recursively Apply the Algorithm:** Set
   $U^{n+1} \leftarrow \tilde{U}_k^n + I_{k+1}^k MG(0, L_{k+1}, I_k^{k+1}(F_k - L_k \tilde{U}_k^n), k+1)$.
4. (optional) **Smooth Again:** Set $U^{n+1} \leftarrow G_k U^{n+1}$.
5. **Return:** Set $MG \leftarrow U^{n+1}$.

As defined algorithm MG is called a symmetric V-cycle if step 4 is used; otherwise algorithm MG is referred to as a *slash* cycle (following the notation of McCormick and Ruge).

For the smoother, G, choose m–applications of damped Jacobi iteration with parameter a. Formally, repeat for $1 \le r \le m$

$$U_j^{r+1} \leftarrow U_j^r + \frac{1}{1+a}(L_{j,j})^{-1}(F - LU^r)_j.$$

The interpolation operator, I_{k+1}^k, is defined as follows. For points common to Ω_{k+1} and to Ω_k set

$$[I_{k+1}^k U]_{2j} = U_j$$

and at odd (new) points of Ω_k require

$$\{L_k[I_{k+1}^k U]\}_{2j-1} = 0.$$

This results in the explicit system of equations at the point x_{2j-1}

$$U_{2j-1}^k = \frac{1}{\beta_{2j-1}^k}\left[\alpha_{2j-1}^k U_{j-1}^{k+1} + \gamma_{2j-1}^k U_{j+1}^{k+1}\right].$$

The restriction operator, I_k^{k+1}, is

$$[I_k^{k+1}U^k]_j = \frac{1}{2}\left[\frac{\alpha_{2j}^k}{\beta_{2j-1}^k}U_{2j-1}^k + U_{2j}^k + \frac{\gamma_{2j}^k}{\beta_{2j+1}^k}U_{2j+1}^k\right].$$

Note that if L_k is symmetric then

$$I_k^{k+1} = \frac{1}{2}(I_{k+1}^k)^T.$$

A fundamental observation due to McCormick and Ruge [McCo82a] in the symmetric case is that S_k can be written

$$S_k = \textit{Range } I_{k+1}^k \oplus \textit{Nullspace } I_k^{k+1}L_k. \tag{9}$$

For non–symmetric problems the above decomposition follows directly from the characterization of *Range* I_{k+1}^k and *Nullspace* $I_k^{k+1}L_k$; see Kamowitz and Parter.

Finally the coarse grid operators, L_{k+1}, are chosen by setting

$$L_{k+1} = \hat{L}_{k+1} \equiv I_k^{k+1}L_k I_{k+1}^k.$$

A direct computation shows that

$$L_{k+1} = \begin{bmatrix} -\alpha_j^{k+1} & \beta_j^{k+1} & -\gamma_j^{k+1} \end{bmatrix}$$

with

$$\alpha_j^{k+1} = \frac{1}{2}\left[\frac{\alpha_{2j}^k \alpha_{2j-1}^k}{\beta_{2j-1}^k}\right] \tag{10}$$

$$\beta_j^{k+1} = \frac{1}{2}\left[\beta_{2j}^k - \frac{\alpha_{2j}^k \gamma_{2j-1}^k}{\beta_{2j-1}^k} - \frac{\gamma_{2j}^k \alpha_{2j+1}^k}{\beta_{2j+1}^k}\right] \tag{11}$$

$$\gamma_j^{k+1} = \frac{1}{2}\left[\frac{\gamma_{2j}^k \gamma_{2j+1}^k}{\beta_{2j+1}^k}\right]. \tag{12}$$

Note that the choice of $\hat{L}_{k+1}$ is the 'natural' choice; however it is not the only feasible choice for L_{k+1}.

3.1 Convergence Theory

For completeness some results from [Kamo85a] are repeated.

Let

$$\epsilon^n = U_{true} - U^n$$

be the error in the nth iterate. Here U_{true} corresponds to the true solution of the algebraic problem

$$L_h U_{true} = f.$$

The rate of improvement of the nth iterate of algorithm MG is then

$$\rho^n = \frac{\|\epsilon^n\|}{\|\epsilon^{n-1}\|}.$$

To estimate ρ, the asymptotic rate as $n \to \infty$, one needs to bound the ρ^n.

For later use define

$$\|x\|_{L_h}^2 \equiv \langle L_h x, x \rangle = \sum_j (L_h x)_j x_j.$$

First the two grid process is considered. Given an initial error

$$\epsilon^0 = U_{true} - U^0,$$

the two grid process yields:

1. Smoothing

$$\epsilon^0 \to \tilde{\epsilon}^0 = G' \epsilon^0$$

where G' corresponds to the linear part of the smoother G. Note that from (9)

$$\tilde{\epsilon}^0 = \eta + I_{2h}^h w_{2h}$$

where

$$\eta \in Nullspace\, I_h^{2h} L_h \text{ and } w_{2h} \in S_{2h}.$$

2. Restricting the residual $r_h = L_h \tilde{\epsilon}^0$ to Ω_{2h} yields

$$R_{2h} = I_h^{2h} L_h \tilde{\epsilon}^0 = I_h^{2h} L_h \eta + I_h^{2h} L_h I_{2h}^h w_{2h} = I_h^{2h} L_h I_{2h}^h w_{2h}$$

since

$$\eta \in Nullspace\, I_h^{2h} L_h.$$

3. Computing the coarse grid correction directly (as is the case for the two grid algorithm) is equivalent to solving

$$L_{2h}\psi_{2h} = R_{2h} = \hat{L}_{2h}w_{2h}.$$

Here

$$L_{2h} = \hat{L}_{2h} = I_h^{2h} L_h I_{2h}^h$$

so

$$\psi_{2h} = w_{2h}.$$

4. Finally, correcting $\tilde{\epsilon}^0$ using the coarse grid correction yields ϵ^1:

$$\begin{aligned} \epsilon^1 &= U_{true} - U^1 \\ &= U_{true} - (\tilde{U}^0 + I_{2h}^h \psi_{2h}) \\ &= \tilde{\epsilon}^0 - I_{2h}^h \psi_{2h} \\ &= \eta + I_{2h}^h w_{2h} - I_{2h}^h \psi_{2h} \\ &= \eta. \end{aligned}$$

Note that if

$$\tilde{\epsilon}^0 \in S_{2h}$$

then one step of the two grid procedure solves the problem! In general, since $\|G'\| \leq 1$ the rate ρ^1 satisfies

$$\rho^1 = \frac{\|\epsilon^1\|}{\|\epsilon^0\|} \leq \frac{\|\epsilon^1\|}{\|\tilde{\epsilon}^0\|}.$$

In this case

$$\epsilon^1 = \eta$$

so

$$\rho^1 = \frac{\|\eta\|}{\|\epsilon^0\|}.$$

Notice that the η term is related to the action of the smoother while the $I_{2h}^h w_{2h}$ term is eliminated by the multigrid process itself.

In Kamowitz and Parter [Kamo85a] an explicit decomposition of S_h was found in terms of the eigenvalues and eigenvectors of the damped Jacobi scheme. This decomposition was exploited to compute bounds on the rate of convergence.

For the two grid scheme, the bounds on ρ, for a given m and a, are given in Table 1. Note that

m	a					
	.333	.500	.667	.750	1.00	1.333
1	.500	.333	.400	.429	.500	.572
2	.250	.111	.160	.184	.250	.326
3	.125	.078	.088	.093	.125	.187
4	.068	.062	.068	.072	.083	.109

Table 1: Predicted Rates for 2 Grids

m	a					
	.333	.500	.667	.750	1.00	1.333
1	.633	.577	.561	.561	.577	.614
2	.435	.408	.417	.424	.447	.475
3	.336	.335	.349	.357	.378	.403
4	.283	.293	.307	.314	.333	.357

Table 2: Predicted Asymptotic Rate

the optimal rate is obtained for $a = .5$. In the succeeding sections the bound in the $a = .5$ case will be obtained experimentally for problems (BL), $(TP\text{-}1)$, and $(TP\text{-}2)$.

In the case where the number of grids is arbitrary, estimates based on the ideas in [McCo82a] are given in Table 2. As indicated in [Kamo85a] these bounds are not sharp.

4 The Singular Perturbation Case

For the study of singular perturbation problems it is necessary that if L_h is an M–matrix then the coarse grid operators L_{k+1}, $k = 1, 2, \ldots$ are also M–matrices. This is necessary to insure that each subproblem

$$L_{k+1}\psi_{k+1} = f_{k+1}$$

is solvable. In particular since the smoother G_{k+1} depends on L_{k+1}, then if L_{k+1} is an M–matrix, $\|G_{k+1}\| < 1$.

Lemma 4.1 *If*

$$L_k = [\ -\alpha_j^k \quad \beta_j^k \quad -\gamma_j^k\ ]$$

is an M-Matrix then

$$L_{k+1} = [\ -\alpha_j^{k+1} \quad \beta_j^{k+1} \quad -\gamma_j^{k+1}\ ]$$

is also an M-matrix, where α_j^{k+1}, β_j^{k+1} and γ_j^{k+1} are given by equations (10–12).

Proof: The hypotheses that L_k is an M-matrix insures that

$$\alpha_j^k > 0, \quad \beta_j^k > 0, \quad \text{and } \gamma_j^k > 0$$

so α_j^{k+1} and γ_j^{k+1} are also positive. In addition, β_j^{k+1} must satisfy

$$\beta_j^{k+1} \geq \alpha_j^{k+1} + \gamma_j^{k+1}.$$

Recalling the expressions for α_j^k, β_j^k and γ_j^k note that this is equivalent to requiring

$$\beta_{2j}^k - \frac{\alpha_{2j}^k \gamma_{2j-1}^k}{\beta_{2j-1}^k} - \frac{\gamma_{2j}^k \alpha_{2j+1}^k}{\beta_{2j+1}^k} \geq \frac{\alpha_{2j}^k \alpha_{2j-1}^k}{\beta_{2j-1}^k} + \frac{\gamma_{2j}^k \gamma_{2j+1}^k}{\beta_{2j+1}^k}$$

or,

$$\beta_{2j}^k \geq \frac{\alpha_{2j}^k}{\beta_{2j-1}^k}\left[\alpha_{2j-1}^k + \gamma_{2j-1}^k\right] + \frac{\gamma_{2j}^k}{\beta_{2j+1}^k}\left[\alpha_{2j+1}^k + \gamma_{2j+1}^k\right]$$

which follows directly from the fact that L_k is diagonally dominant.

Since each of the L_{k+1} is an M–matrix, the theory developed in Section 3.1 can be applied in the singular perturbation case.

5 Experimental Results

The algorithm of the previous sections was applied to problems (*BL*), (*TP-1*) and (*TP-2*). Problem (*BL*) exhibits a boundary layer at $x = 1$. From a computational point of view the system of linear equations that is solved is well conditioned even for small ε; however the fact that the linear system is not symmetric leads to computational difficulties in computing the experimental rate of convergence.

In the case of problem (*TP-1*) there are two boundary layers; at $x = 0$ and at $x = 1$. In addition the system of equations that is solved is ill–conditioned.

The discrete problem corresponding to problem (*TP-2*) is well conditioned. The fact that there is an interior turning point at $x = 1/2$ does not appear to lead to computational difficulties.

By using the one sided difference schemes discussed in the previous section the linear systems arising from the discretization of the problems are of positive type.

From a practical standpoint, however, what effect does the ill–conditioning have on the observed solution? In particular, how should the rate of convergence (reduction in the error) be measured?

5.1 General Remarks Regarding the Experiments

In all the experiments N, the number of points on the fine grid, was 63. The initial guess, U^0, was constructed so that the initial error could be chosen in advance. In other words,

$$U_j^0 = u(x_j) - \epsilon_j.$$

For the experiments discussed here

$$\epsilon_j = (-1)^j.$$

The number of smoothing steps for the experiments discussed here was set to one. Experiments were run where the number of smoothing steps was greater than one. When more than one smoothing step was used there was no observed qualitative difference in the behavior of the algorithm compared to the behavior for non-singular perturbation problems. Unless otherwise noted the results are for the two grid case. The computer used was a VAX-11/780 and the tests were run in double precision (roughly 16 decimal digits of accuracy).

The damped Jacobi parameter, a, was chosen to be .5. The following heuristic argument due to Brandt [Bran77a] suggests why $a = .5$ is optimal for one smoothing step. His suggestion is to choose a so that the range of eigenvalues which are reduced by the damped Jacobi process is equal to the range which is left alone by the process. As noted in [Kamo85a] the eigenvalues of the damped Jacobi scheme come in pairs $\lambda(\mu)$ and $\hat{\lambda}(\mu)$ where

$$\lambda(\mu) = \frac{\mu + a}{1 + a} \quad \text{and} \quad \hat{\lambda}(\mu) = \frac{a - \mu}{1 + a}$$

and μ are the eigenvalues of the scheme for $a = 0$. The eigenvalues μ are real and distinct and as $h \to 0$ they fill out the interval $[0, 1]$. Brandt's requirement corresponds to choosing a so that

$$-\lambda(-1) = \lambda(0)$$

or in other words to taking $a = 1/2$. Note that this is equivalent to requiring

$$-\hat{\lambda}(1) = \hat{\lambda}(0).$$

Indeed in [Kamo85a] for 1 smoothing step the theoretical and experimental results indicate that this choice of a is optimal.

5.2 Results for the Boundary Layer Problem

For problem (BL) the solution to the analytic problem can be calculated explicitly. For all $\varepsilon > 0$ the solution $u_\varepsilon(x)$ is

$$u_\varepsilon(x) = C_1 e^{x/\varepsilon} + C_2.$$

Grid	ε						
	1	.1	.01	.005	.003	.001	0
1	$.62 \times 10^{-3}$	$.11 \times 10^{-2}$	$.54 \times 10^{-2}$	$.73 \times 10^{-2}$	$.86 \times 10^{-2}$	.011	.012
2	$.25 \times 10^{-2}$	$.45 \times 10^{-2}$	$.18 \times 10^{-1}$	$.21 \times 10^{-1}$	$.28 \times 10^{-1}$	.027	.024
3	$.98 \times 10^{-2}$	$.12 \times 10^{-1}$	$.37 \times 10^{-1}$	$.44 \times 10^{-1}$	$.46 \times 10^{-1}$	.048	.048
4	$.39 \times 10^{-1}$	$.41 \times 10^{-1}$	$.80 \times 10^{-1}$	$.92 \times 10^{-1}$	$.96 \times 10^{-1}$	.099	.1
5	.15	.15	.19	.20	.21	.21	.21
6	1	1	1	1	1	1	1

Table 3: Condition Number – Problem *BL*

The constants C_1 and C_2 satisfy

$$C_1 = \frac{2}{e^{1/\varepsilon} - 1}, \qquad C_2 = 1 - C_1 = \frac{e^{1/\varepsilon} - 3}{e^{1/\varepsilon} - 1}.$$

Note that

$$\lim_{\varepsilon \to 0} C_1 = 0, \qquad \lim_{\varepsilon \to 0} C_2 = 1$$

so

$$\lim_{\varepsilon \to 0} u_\varepsilon(x) = 1.$$

Denote by $U_{h,\varepsilon}(x)$ the numerical solution of problem (BL) for a fixed h and ε. The consistency condition on the solution then requires that for fixed ε

$$\lim_{h \to 0} U_{h,\varepsilon}(x) = u_\varepsilon(x).$$

Dorr [Dorr70a] proved that for fixed h

$$\lim_{\varepsilon \to 0} U_{h,\varepsilon}(x) = 1.$$

The discretization of problem (BL) using L_h^1 (standard upwind differencing) results in an approximation to the true solution which is an $O(h)$ approximation. To improve on this approximation Kellogg and Tsan point out that the use of L_h^2 results in an $O(h^2)$ approximation for $\varepsilon > 0$. For the reduced problem ($\varepsilon = 0$) L_h^2 gives an $O(h)$ approximation.

It is important to note that the linear system of equations arising from the discretization of Problem (BL) is not ill-conditioned. Table 3 displays the LINPACK [Dong79a] estimate RCOND (an estimate of the inverse of the condition number) for L_h^1, $h = 1/64$ and $\varepsilon = 1$, .01, .005, .003, and .001.

First, some general conclusions about the experimental results. For both L_h^1 and L_h^2 the algorithm converged to the solution of the algebraic problem with an asymptotic convergence rate

identical to the rate predicted in Section 3.1. Moreover there was no observed qualitative difference in the behavior of the algorithm with respect to the choice of L_h^1 or L_h^2. However, as $\varepsilon \to 0$ the behavior of the iterates changes dramatically.

Define

$$R_n = \frac{\|r_n\|}{\|r_{n-1}\|}$$

where

$$r_n = F - L_h U^n$$

is the residual after the nth iteration and the norm used is the l_2 norm. From a computational point of view this is a convenient measure of the rate of improvement since one does not know the true solution. From past computational experience this ratio is bounded above by the theoretical error reduction rate. Indeed for large ε, say $\varepsilon = 1$, this is the case. For small ε, say $\varepsilon = .001$, after a small number of iterations R_n exceeded the rate predicted in Table 1, and then as n increased R_n declined towards the predicted rate; see the solid line in Figure 1. The dashed line will be referred to later. In both cases two grids are used.

An explanation for this behavior is that as the algorithm proceeds the fact that the error is being measured in an asymmetric norm causes problems. The user of the algorithm should be careful to note that while in principle all norms on finite dimensional spaces are equivalent the use of a symmetric norm results in much better observed behavior of this particular algorithm.

To demonstrate this hypothesis the problem

$$L_h U = F$$

is transformed into the equivalent symmetric problem

$$D^{-1} L_h D (D^{-1} U) = D^{-1} F = \hat{F}. \tag{13}$$

The matrix D is a positive diagonal matrix whose entries are given by

$$d_1 = 1, \qquad d_i = \sqrt{\frac{\alpha_i}{\gamma_{i-1}}} d_{i-1}.$$

Applying this transformation to L_h results in L_h^s which is now symmetric. The matrix L_h^s is denoted

$$L_h^s = [\ -\alpha_i d_{i-1}/d_i \quad \beta_i \quad -\gamma_i d_{i+1}/d_i\ ].$$

Denote by algorithm MG^s algorithm MG applied to problem (13). The error resulting from applying algorithm MG^s is related to the error from applying algorithm MG as follows:

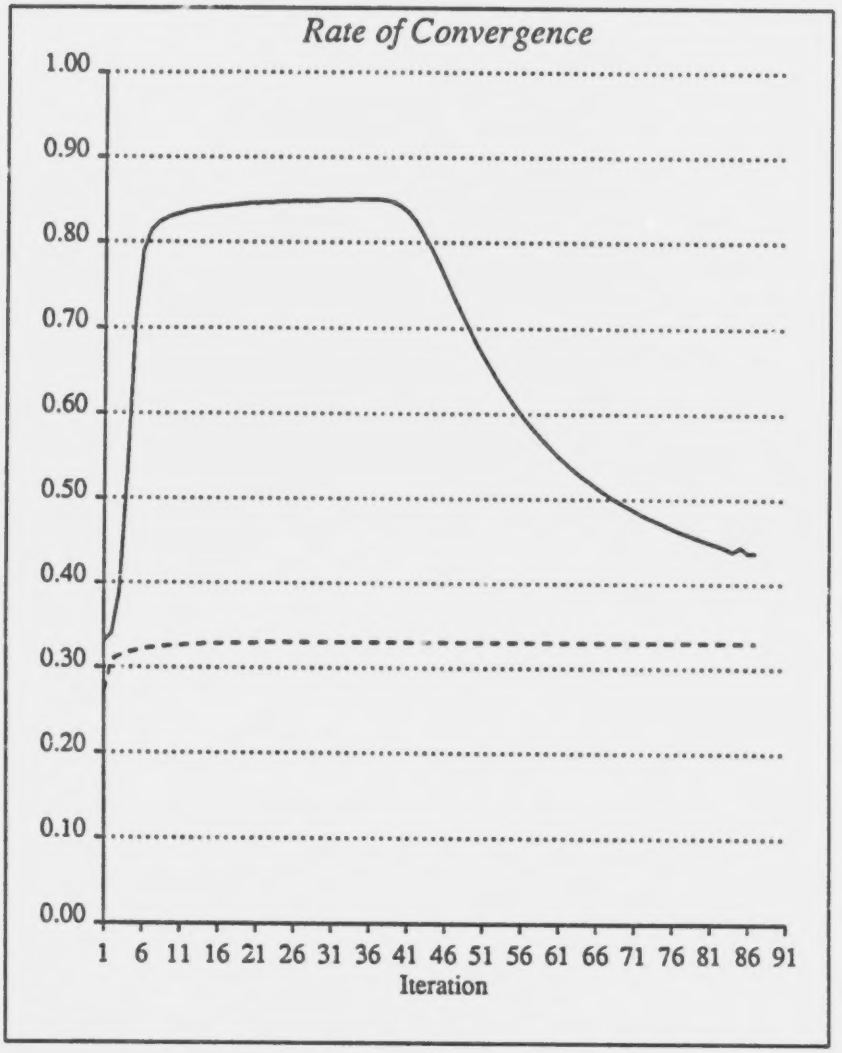

Figure 1: R_n, for $\epsilon = .001$

Lemma 5.1 *If ϵ^n is the error after the nth iteration of applying algorithm MG then the new error, ϵ^{n+1}, is related to the error in the symmetric problem by*

$$(MG^s)(D^{-1}\epsilon) = D^{-1}MG\epsilon = D^{-1}\epsilon^{n+1}.$$

Proof: By the definition of ϵ^n,

$$\epsilon^n = U - U^n$$

and

$$\epsilon^{n+1} = U - U^{n+1} = MG\epsilon^n.$$

Also,

$$D^{-1}\epsilon^n = D^{-1}U - D^{-1}U^n.$$

Applying each step of algorithm MG^s to $D^{-1}U^n$ results in $D^{-1}U^{n+1}$ as a straightforward calculation shows. Hence

$$MG^s\ D^{-1}U^n = D^{-1}MG\ U^n.$$

Applying this transformation to the error ϵ^n and computing the rates

$$D^{-1}R_n = \frac{\|D^{-1}\epsilon^n\|_{L_h}}{\|D^{-1}\epsilon^{n-1}\|_{L_h}}$$

results in the more usual behavior displayed by the dashed line in Figure 1. Figure 2 displays the location where the maximum norm of the error is taken on versus the iteration number. Notice how as the iteration proceeds the location where the maximum occurs 'drifts.' Applying D^{-1} and then measuring R_n has the effect of 'fixing' the location where the maximum error is taken on.

Unfortunately the entries of the transformation matrix D satisfy

$$D_i \to \infty$$

as $\varepsilon \to 0$ so this is not a stable method for solving this problem in general.

In summary, for problem (2) where the coefficient matrix was not poorly conditioned but was non–symmetric the only computational difficulty was in choosing the norm in which to measure the rate of improvement of the algorithm.

5.3 Turning point Problem – 1

In this section consider the solution of

$$-\varepsilon u_\varepsilon'' + (x - \frac{1}{2})u_\varepsilon' = 0, \tag{14}$$

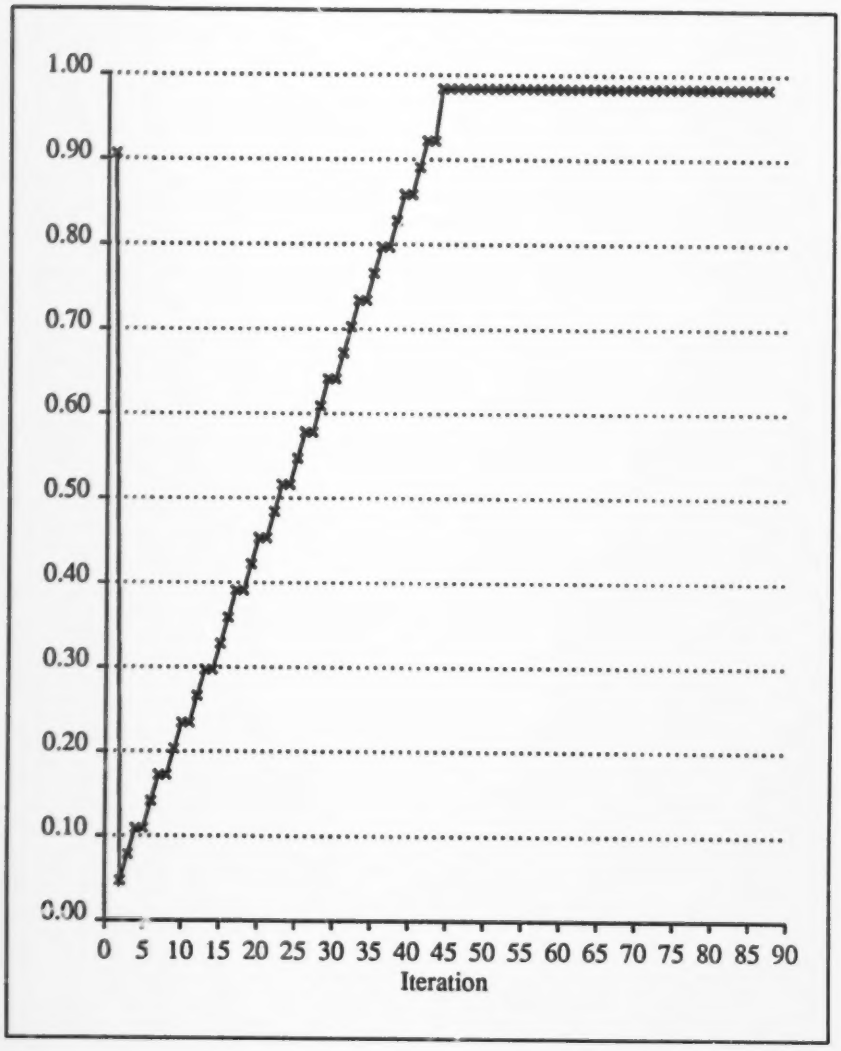

Figure 2: Index of Maximum Error, Problem *BL*

Grid	ε					
	1	.1	.01	.005	.003	.001
1	.00023	.00032	$.20 \times 10^{-6}$	$.19 \times 10^{-9}$	$.13 \times 10^{-12}$	$.71 \times 10^{-21}$
2	.0023	.0013	$.76 \times 10^{-6}$	$.66 \times 10^{-9}$	$.41 \times 10^{-12}$	$.23 \times 10^{-18}$
3	.0096	.0085	$.83 \times 10^{-2}$	$.85 \times 10^{-2}$	$.80 \times 10^{-2}$	$.60 \times 10^{-2}$
4	.038	.037	$.46 \times 10^{-1}$	$.55 \times 10^{-1}$	$.60 \times 10^{-1}$	$.65 \times 10^{-1}$
5	.15	.146	.16	.17	.18	.19
6	1	1	1	1	1	1

Table 4: Condition Number – Problem *TF-1*

with

$$u_\varepsilon(0) = 1, \qquad u_\varepsilon(1) = 3.$$

This problem has two boundary layers, at $x = 0$ and at $x = 1$. The asymptotic solution satisfies (see [Krei74a] and [Dorr70a])

$$\lim_{\varepsilon \to 0} u_\varepsilon(x) = 2.$$

For the discrete problem again

$$L_h^3 U = F \tag{15}$$

is solved where L_h^3 is given by equations (5) and (6). The condition number of L_h^3 tends to infinity as $\varepsilon \to 0$ for a fixed h. Table 4 displays the LINPACK estimate RCOND for L_h^3, $h = 1/64$ and $\varepsilon = 1$, .01, .005, .003, and .001. It is important to note that although the operator corresponding to the original discretization on the h–grid is ill–conditioned, L_k, $k = 3, 4, \ldots$ are not ill–conditioned. In fact in the limiting case where the coarse grid has one point the system of equations to be solved is a 1×1 system which has condition number 1. This feature of the multigrid algorithm is reassuring to the user since it means that the actual system being solved directly in step 1 of algorithm *MG* is well conditioned and no special measures need to be taken.

Although the coarse grids used in the algorithm do not resolve the boundary layers the algorithm still converges. This is because the role of the coarse grids is to solve for the error in the solution, rather than to represent the solution itself. The boundary layers are not seen in the expression for the error. The observed rate of convergence was independent of the value of ε used.

For all tested values of ε the multigrid algorithm converged to the solution computed by Gaussian Elimination to the algebraic problem. However, the ill–conditioning of the algebraic system resulting from the discretization of the continuous problem opens up the question of to what solution does the multigrid algorithm converge? Since the original system is ill–conditioned there is a family of solutions U for which the residual is small. Indeed for $\varepsilon = .001$ the condition number

Grid	ε						
	1	.1	.01	.005	.003	.001	0
1	$.64 \times 10^{-3}$	$.98 \times 10^{-3}$	$.45 \times 10^{-2}$	$.69 \times 10^{-2}$	$.89 \times 10^{-2}$	.013	0
2	$.26 \times 10^{-2}$	$.39 \times 10^{-2}$	$.17 \times 10^{-1}$	$.24 \times 10^{-1}$	$.28 \times 10^{-1}$	.031	0
3	$.99 \times 10^{-2}$	$.11 \times 10^{-1}$	$.25 \times 10^{-1}$	$.33 \times 10^{-1}$	$.37 \times 10^{-1}$	.038	.035
4	.039	.040	.063	.080	.089	.095	.096
5	.15	.15	.18	.20	.21	.22	.22
6	1	1	1	1	1	1	1

Table 5: Condition Number – Problem *TP-2*

estimate is $.71 \times 10^{-21}$ which is less than the unit roundoff of the VAX-11/780. Thus there is no reason to expect that the solution calculated by solving equation (15) is an adequate approximation to the solution of the continuous problem. In the experimental runs that was indeed the case and both algorithm *MG* and Gaussian Elimination returned 0 for the solution.

Since for this problem the error is not skewed as in problem (*BL*), it is not surprising to see that the ratio of improvements R_n are bounded above by the predicted rate from Table 1. This can be seen in Figure 3, for $\varepsilon = .001$.

5.4 Turning point Problem – 2

In this section the solution to

$$-\varepsilon u_\varepsilon'' - (x - \frac{1}{2})u_\varepsilon' = 0, \tag{16}$$

is discussed. The asymptotic solution, see [Krei74a] is

$$\begin{aligned} u_\varepsilon(x) &= 1, \qquad 0 \le x \le \frac{1}{2} \\ u_\varepsilon(x) &= 3, \qquad \frac{1}{2} \le x \le 1. \end{aligned}$$

Although one sided differencing, in this case L_h^4, is used to compute the solution, the system of equations that is solved is not ill-conditioned. As in Section 5.3 the LINPACK estimate RCOND of the condition number was computed; see Table 5.

It appears that the condition number is related to the boundary data. For problem (*TP-1*) the discretization uses information from the boundary layer to estimate $u_\varepsilon(x)$ at interior points. The boundary data for problem (*TP-2*) is well represented (no boundary layers) in the interior.

From the standpoint of the multigrid algorithm again as the grids get coarser the condition number improves. Also, as for problem (*TP-1*) the rate of convergence of the algorithm was

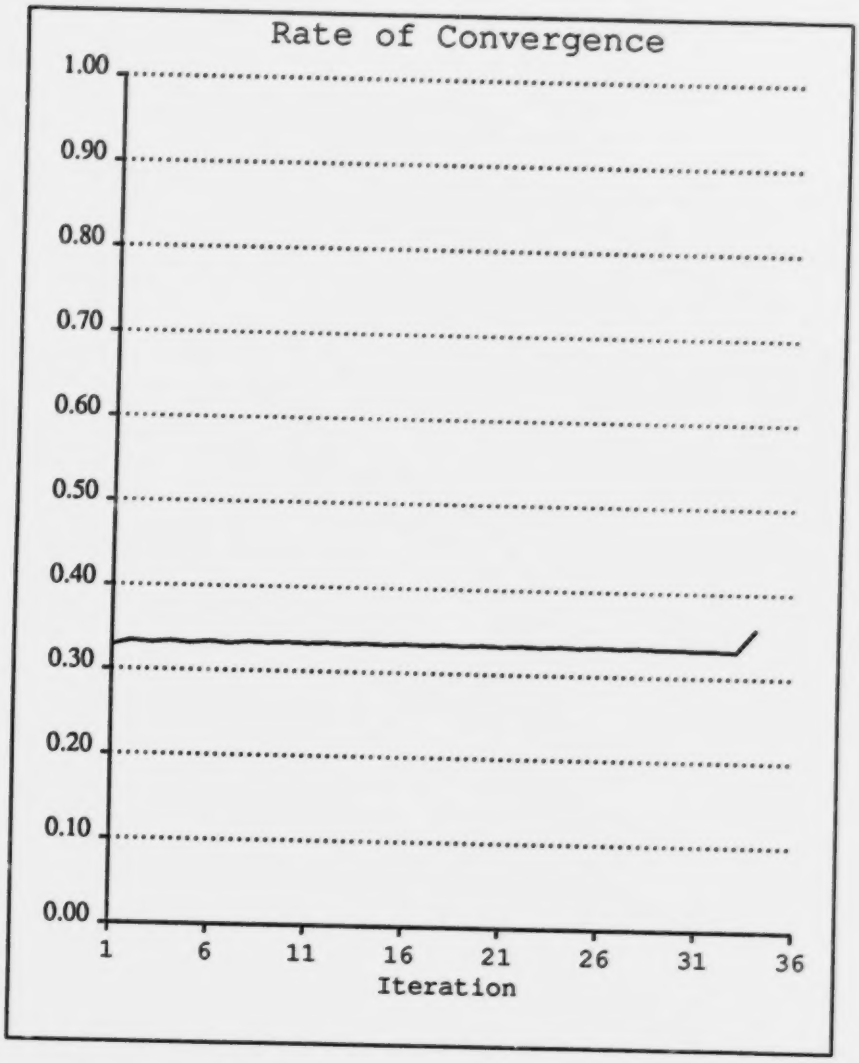

Figure 3: R_n – Problem *TP-1*, $\varepsilon = .001$

independent of the value of ε, and was identical to the rate predicted in Section 3.1. In addition R_n was bounded above by the predicted rate.

6 Comparison of $I_h^{2h} L_h I_{2h}^h$ and L_{2h}

From a computational point of view one would like to choose for the coarse grid operator L_{2h} the tridiagonal operator analogous to L_h obtained by finite differences. This choice for L_{2h} will be denoted L_{2h}^{fd}. For now only the *symmetric* problem

$$-(pu')' = f, \qquad p(x) \geq p_0 > 0 \tag{17}$$

with boundary conditions

$$u(0) = u(1) = 0$$

is considered. Here $p(x)$ is a smooth function.

Lemma 6.1 *The operator L_{2h}^{fd} is related to $\hat{L}_{2h}$ by*

$$\hat{L}_{2h} = L_{2h}^{fd} + h^2 [\ -A_j \quad B_j \quad -C_j\ ]$$

where A_j, C_j depend on $p(x)$, $p'(x)$ and $p''(x)$, and $B_j = A_j + C_j$.

Proof: Recall that the coefficients of $\hat{L}_{2h}$ are given in equations (10-12). In particular

$$\hat{\alpha}_k = \frac{1}{2}\left[\frac{\alpha_{2k}\alpha_{2k-1}}{\beta_{2k-1}}\right].$$

Expanding

$$\begin{aligned}
\alpha_{2k} &= p(\frac{4k-1}{2}h), \\
\alpha_{2k-1} &= p(\frac{4k-3}{2}h) \qquad \text{and} \\
\beta_{2k-1} &= p(\frac{4k-1}{2}h) + p(\frac{4k-3}{2}h)
\end{aligned}$$

in Taylor series about the point $\bar{x} = (4k-1)h$ and collecting terms yields

$$\begin{aligned}
\hat{\alpha}_k &= \frac{1}{2}\frac{\alpha_{2k}\alpha_{2k-1}}{\beta_{2k-1}} \\
&= \frac{1}{2}\frac{p((\frac{4k-1}{2})h)p((\frac{4k-3}{2})h)}{p((\frac{4k-1}{2})h) + p((\frac{4k-3}{2})h)}
\end{aligned}$$

$$
\begin{aligned}
&= \frac{1}{2}\frac{[p(\bar{x})+\frac{h}{2}p'(\bar{x})+\frac{h^2}{8}p''(\bar{x})+C_1h^3][p(\bar{x})-\frac{h}{2}p'(\bar{x})+\frac{h^2}{8}p''(\bar{x})-C_2h^3]}{[p(\bar{x})+\frac{h}{2}p'(\bar{x})+\frac{h^2}{8}p''(\bar{x})+C_1h^3]+[p(\bar{x})-\frac{h}{2}p'(\bar{x})+\frac{h^2}{8}p''(\bar{x})-C_2h^3]} \\
&= \frac{1}{2}\frac{p(\bar{x})^2+h^2[\frac{1}{4}p''(\bar{x})p(\bar{x})-\frac{1}{4}(p'(\bar{x}))^2]+Dh^3}{2p(\bar{x})+\frac{h^2}{4}p''(\bar{x})+Eh^3} \\
&= \frac{1}{4}p(\bar{x})+h^2A_k \\
&= \alpha_k^{fd}+h^2A_k
\end{aligned}
$$

where A_k depends on $p(\bar{x})$, $p'(\bar{x})$ and $p''(\bar{x})$.

A similar calculation yields

$$\hat{\gamma}_k = \gamma_k^{fd} + h^2C_k.$$

In addition

$$
\begin{aligned}
\hat{\beta}_k &= \hat{\alpha}_k + \hat{\gamma}_k \\
&= \alpha_k^{fd} + h^2A_k + \gamma_k^{fd} + h^2C_k \\
&= \beta_k^{fd} + h^2B_k.
\end{aligned}
$$

The error analysis in Section 3.1 shows that if $\hat{L}_{2h}$ is not used then the coarse grid correction ψ_{2h} will not equal w_{2h}. Thus a bound on the eigenvalues of the eigenvalue problem

$$\lambda L_{2h}^{fd}\psi = \hat{L}_{2h}\psi$$

is needed.

Lemma 6.2 *The eigenvalues λ of*

$$\lambda L_{2h}^{fd}\psi = \hat{L}_{2h}\psi$$

satisfy

$$|\lambda - 1| \leq \frac{\max|C_i|}{\min|\hat{\gamma}_i|}h^2 < \infty.$$

Proof: By Lemma 6.1

$$\hat{L}_{2h} = L_{2h}^{fd} + h^2[\ -A_j \quad B_j \quad -C_j\ ],$$

thus

$$(\lambda-1)\langle L_{2h}^{fd}\psi,\psi\rangle = h^2\langle[\ -A_i \quad B_i \quad -C_i\ ]\psi,\psi\rangle.$$

Summation by parts yields

$$\begin{aligned}
\lambda - 1 &= h^2 \frac{\langle [\ -A_i \quad B_i \quad -C_i\ ]\psi, \psi\rangle}{\langle L_{2h}^{fd}\psi, \psi\rangle} \\
&= h^2 \frac{\sum C_i(\psi_i - \psi_{i+1})^2}{\sum \gamma_i^{fd}(\psi_i - \psi_{i+1})^2} \\
&\leq h^2 \frac{\max|C_i|}{\min|\gamma_i^{fd}|} \\
&= Kh^2 \\
&< \infty
\end{aligned}$$

because of the smoothness of p and since $|\gamma_i^{fd}| \geq p_0 > 0$. In addition, since L_{2h}^{fd} is positive definite,

$$(\lambda - 1)\langle L_{2h}^{fd}\psi, \psi\rangle > 0$$

which implies

$$\lambda - 1 \geq -Kh^2.$$

Therefore

$$|\lambda - 1| \leq Kh^2.$$

Recall from equation (9)

$$\tilde{\epsilon}^0 = \eta + I_{2h}^h w_{2h}$$

and if $\hat{L}_{2h}$ is used then

$$\epsilon^1 = \eta.$$

In the case where L_{2h}^{fd} is used to solve

$$L_{2h}^{fd}\psi_{2h} = \hat{L}_{2h}w_{2h}$$

the error is denoted $\bar{\epsilon}^1$. Now

$$\bar{\epsilon}^1 = \eta + I_{2h}^h(w_{2h} - \psi_{2h}).$$

Since *Range* I_{2h}^h and *Nullspace* $I_h^{2h}L_h$ are L_h—orthogonal (see [Kamo85a]),

$$\|\bar{\epsilon}^1\|_{L_h}^2 = \|\eta\|_{L_h}^2 + \|I_{2h}^h(w_{2h} - \psi_{2h})\|_{L_h}^2.$$

Applying Lemmas 6.1 and 6.2,

$$\begin{aligned}
\|I_{2h}^h(w_{2h}-\psi_{2h})\|_{L_h}^2 &= \langle L_h I_{2h}^h(w_{2h}-\psi_{2h}), I_{2h}^h(w_{2h}-\psi_{2h})\rangle \\
&= \frac{1}{2}\langle \hat{L}_{2h}(w_{2h}-\psi_{2h}),(w_{2h}-\psi_{2h})\rangle \\
&= \frac{1}{2}\langle \hat{L}_{2h}(w_{2h}-(L_{2h}^{fd})^{-1}\hat{L}_{2h}w_{2h}),(w_{2h}-(L_{2h}^{fd})^{-1}\hat{L}_{2h}w_{2h})\rangle \\
&= \frac{1}{2}\langle F\hat{L}_{2h}^{1/2}w_{2h}, F\hat{L}_{2h}^{1/2}w_{2h}\rangle
\end{aligned}$$

where

$$F = (I - \hat{L}_{2h}^{1/2}(L_{2h}^{fd})^{-1}\hat{L}_{2h}^{1/2}).$$

The eigenvalues of $\hat{L}_{2h}^{1/2}(L_{2h}^{fd})^{-1}\hat{L}_{2h}^{1/2}$ are the same as the eigenvalues of $(L_{2h}^{fd})^{-1}\hat{L}_{2h}$, so by Lemma 6.2

$$\begin{aligned}
\frac{1}{2}\langle F\hat{L}_{2h}^{1/2}w_{2h}, F\hat{L}_{2h}^{1/2}w_{2h}\rangle &\le \frac{1}{2}(Kh^2)^2\langle \hat{L}_{2h}^{1/2}w_{2h}, \hat{L}_{2h}^{1/2}w_{2h}\rangle \\
&= \frac{1}{2}(Kh^2)^2\langle \hat{L}_{2h}w_{2h}, w_{2h}\rangle \\
&= (Kh^2)^2\langle L_h I_{2h}^h w_{2h}, I_{2h}^h w_{2h}\rangle.
\end{aligned}$$

Therefore

$$\|I_{2h}^h(w_{2h}-\psi_{2h})\|_{L_h}^2 \le (Kh^2)^2\|I_{2h}^h w_{2h}\|_{L_h}^2$$

and

$$\|\bar{\epsilon}^1\|_{L_h}^2 \le \|\eta\|_{L_h}^2 + (Kh^2)^2\|I_{2h}^h w_{2h}\|_{L_h}^2.$$

Since $\|G\|_{L_h} \le 1$,

$$\|\bar{\epsilon}^1\|_{L_h} \le \|\eta\|_{L_h} + Kh^2\|\epsilon^0\|_{L_h}.$$

Finally, the rate using L_{2h}^{fd} is

$$\begin{aligned}
\rho^{fd} &= \frac{\|\bar{\epsilon}^1\|_{L_h}}{\|\epsilon^0\|_{L_h}} \\
&\le \frac{\|\eta\|_{L_h}}{\|\epsilon^0\|_{L_h}} + Kh^2.
\end{aligned}$$

Recall the rate using $\hat{L}_{2h}$ is

$$\rho \le \frac{\|\eta\|_{L_h}}{\|\epsilon^0\|_{L_h}}$$

so

$$\rho^{fd} \leq \rho + Kh^2.$$

Remark: Although the discussion in the previous section is restricted to symmetric problems, the same result extends to the general two point boundary value problem

$$-(pu')' + bu' + cu = f, \qquad p(x) \geq p_0 > 0, c(x) \geq 0 \tag{18}$$

since problem (18) can be rewritten

$$-(\bar{p}u')' + \bar{c}u = \bar{f} \tag{19}$$

where

$$\bar{p} = g(x), \tag{20}$$

$$\bar{c} = g(x)\frac{c(x)}{p(x)} \tag{21}$$

$$\bar{f} = g(x)\frac{f(x)}{p(x)}. \tag{22}$$

The function $g(x)$ is

$$g(x) = exp\{-\int \frac{b(x) - p'(x)}{p(x)}dx\}.$$

Note that $\bar{p}$, $\bar{c}$ and $\bar{f}$ are defined since

$$p(x) \geq p_0 > 0.$$

6.1 An Illustration

As an illustration of the effect of replacing $\hat{L}_{2h}$ with L_{2h}^{fd} consider using for the smoother G in algorithm MG one sweep of odd Gauss-Seidel smoothing. In other words

$$(GU)_i = U_i \qquad \text{for } i = 0 \bmod 2$$

and for $i = 1 \bmod 2$

$$(GU)_i = \frac{1}{\beta_i}[\alpha_i U_{i-1} + \gamma_i U_{i+1} + f_i].$$

This guarantees that the error $\tilde{\epsilon}$ lies completely in $RangeI_{2h}^{h}$. In other words, the η term is 0 since for $i = 0 \bmod 2$

$$(L_h I_{2h}^{h} w_{2h})_i \neq 0$$

yet

$$\begin{aligned} 0 &= \langle L_h \eta, I_{2h}^h w_{2h} \rangle \\ &= \langle \eta, L_h I_{2h}^h w_{2h} \rangle. \end{aligned}$$

In addition for points x_i, with $i = 1 \bmod 2$,

$$\begin{aligned} 0 = r_i = L_h \tilde{\epsilon} &= (L_h \eta)_i + (L_h I_{2h}^h w_{2h})_i \\ &= (L_h \eta)_i \end{aligned}$$

which implies $\eta_i = 0$ since $\eta_{i-1} = \eta_{i+1} = 0$.

Thus

$$\tilde{\epsilon} = I_{2h}^h w_{2h}$$

for some w_{2h}. If $\hat{L}_{2h}$ is used then one iteration of the algorithm results in completely solving the problem.

For a numerical example problem (17) is solved with

$$p(x) = e^{\cos(\pi x)}.$$

The right hand side f is chosen so that the the true solution is

$$u_{true}(x) = \sin(\pi x).$$

As expected when $\hat{L}_{2h}$ is used the algorithm converges in one step. When L_{2h}^{fd} is used then the observed rate of convergence corresponds to the Kh^2 term of Section 6. Table 6 displays the observed rate of convergence versus h for four different choices for the number of grids. The column $\rho(h)$ corresponds to the observed rate of convergence for each value of h. The value of $\delta(h)$ is

$$\delta(h) = \frac{\rho(2h)}{\rho(h)}.$$

Since the error in the two grid case is $O(h^2)$ one expects that $\delta(h) \to 4$ as $h \to 0$ for two grids. Indeed this is the case. The reason why $\rho(h)$ varies with the number of grids used is that there are 'pollution' effects from not solving each coarse grid equation exactly. In other words

$$\epsilon^1 = \eta_h + I_{2h}^h \eta_{2h} + \ldots + O(h^2),$$

where the $O(h^2)$ term corresponds to the error made by not using $\hat{L}_{2h}$.

	2 grids		3 grids		4 grids		5 grids	
h	$\rho(h)$	$\delta(h)$	$\rho(h)$	$\delta(h)$	$\rho(h)$	$\delta(h)$	$\rho(h)$	$\delta(h)$
1/16	$.50 \times 10^{-2}$		$.27 \times 10^{-1}$		$.85 \times 10^{-1}$			
1/32	$.12 \times 10^{-2}$	4.17	$.62 \times 10^{-2}$	4.35	$.28 \times 10^{-1}$	3.04	$.86 \times 10^{-1}$	
1/64	$.30 \times 10^{-3}$	4.00	$.15 \times 10^{-2}$	4.13	$.65 \times 10^{-2}$	4.31	$.29 \times 10^{-1}$	3.01
1/127	$.75 \times 10^{-4}$	4.00	$.38 \times 10^{-3}$	3.95	$.16 \times 10^{-2}$	4.06	$.66 \times 10^{-2}$	4.33

Table 6: Rate using L_{2h}^{fd}

Acknowledgements. The author is indebted to Seymour Parter for many interesting discussions and to Naomi Decker and Bob Voigt for their careful readings of the manuscript.

7 References

[Babu69a] **Babuska, I.**, "Numerical Stability in the Solution of the Tri-diagonal Matrices," Technical Note BN-609, University of Maryland, June 1969.

[Berm79a] **Berman, A. and R. Plemmons**, *Nonnegative Matrices in the Mathematical Sciences*, Academic Press, New York, 1979.

[Bran77a] **Brandt, A.**, "Multilevel Adaptive Solutions to Boundary-value Problems," *Math. Comp.* 31 (1977), pp. 333-390.

[Dong79a] **Dongarra, J.J., J.R. Bunch, C.B. Moler, and G.W. Stewart**, *Linpack User's Guide*, SIAM, Philadelphia, 1979.

[Dorr70a] **Dorr, F.**, "An Example of Ill-Conditioning in the Numerical Solution of Singular Perturbation Problems," Technical Report 4361, Los Alamos Scientific Laboratory, February 1970.

[Ervi85a] **Ervin, V. and W. Layton**, "A Second Order Accurate, Positive Scheme for Singularly Perturbed Boundary Value Problems," Preliminary Report, Georgia Institute of Technology, March 1985.

[Kamo85a] **Kamowitz, D. and S. V. Parter**, "A Study of Some Multigrid Ideas," *Applied Mathematics and Computation* 17 (1985), pp. 153-184.

[Kell78a] **Kellogg, R. and A. Tsan**, "Analysis of Some Difference Approximations for a Singular Perturbation Problem Without Turning Points," *Math. Comp.* 32 (1978), pp. 1025-1039.

[Krei74a] **Kreiss, H. O. and S. V. Parter**, "Remarks on Singular Perturbations with Turning Points," *SIAM Journal of Numerical Analysis* 5 (1974), pp. 230-251.

[McCo82a] **McCormick, S. and J. Ruge**, "Multigrid Methods for Variational Problems," *SIAM Journal of Numerical Analysis* 19 (1982), pp. 924-929.

Standard Bibliographic Page

1. Report No. NASA CR-178230 ICASE Report No. 87-1	2. Government Accession No.	3. Recipient's Catalog No.
4. Title and Subtitle MULTIGRID APPLIED TO SINGULAR PERTURBATION PROBLEMS		5. Report Date January 1987
		6. Performing Organization Code
7. Author(s) David Kamowitz		8. Performing Organization Report No. 87-1
9. Performing Organization Name and Address Institute for Computer Applications in Science and Engineering Mail Stop 132C, NASA Langley Research Center Hampton, VA 23665-5225		10. Work Unit No. 11. Contract or Grant No. NAS1-18107
12. Sponsoring Agency Name and Address National Aeronautics and Space Administration Washington, D.C. 20546		13. Type of Report and Period Covered Contractor Report 14. Sponsoring Agency Code 505-90-21-01

15. Supplementary Notes

Langley Technical Monitor:
J. C. South

Submitted to Applied Mathematics and Computation

Final Report

16. Abstract

The solution of the singular perturbation problem

$$-\varepsilon u'' + b(x)u' = f, \qquad 0 < x < 1$$

with

$$1 \gg \varepsilon > 0, \quad u(0) = u_0, \quad u(1) = u_1$$

by a multigrid algorithm is considered. Theoretical and experimental results for a number of different discretizations are presented. The theoretical and observed rates agree with the results developed in an earlier work of Kamowitz and Parter.

In addition, the rate of convergence of the algorithm when the coarse grid operator is the natural finite difference analogue of the fine grid operator is presented. This is in contrast to the case in the previous work where the Galerkin choice ($I_h^H L_h I_H^h$) was used for the coarse grid operators.

17. Key Words (Suggested by Authors(s))	18. Distribution Statement
multigrid, singular perturbation	61 - Computer Programming and Software 64 - Numerical Analysis Unclassified - unlimited

19. Security Classif.(of this report)	20. Security Classif.(of this page)	21. No. of Pages	22. Price
Unclassified	Unclassified	27	A03

For sale by the National Technical Information Service, Springfield, Virginia 22161

NASA-Langley, 1987